https://doi.org/10.20965/jrm.2021.p0329

Paper:

Small Flying Object Classifications Based on Trajectories and Support Vector Machines

Jalvin Jia Xiang Chan*, Sutthiphong Srigrarom*, Jiawei Cao, Pengfei Wang**, and Photchara Ratsamee*****

*Department of Mechanical Engineering, National University of Singapore
9 Engineering Drive 1, Block EA #07-08 117575, Singapore
E-mail: E0202866@u.nus.edu, spot.srigrarom@nus.edu.sg
**Temasek Laboratories, National University of Singapore
T-Lab Building, 5A Engineering Drive 1, #09-02 117411, Singapore
E-mail: {tslcaoj, tslwpf}@nus.edu.sg
***Cyber Media Center, Osaka University
5-1 Mihogaoka, Ibaraki, Osaka 567-0047, Japan
E-mail: photchara@ime.cmc.osaka-u.ac.jp
[Received October 9, 2020; accepted February 18, 2021]

This paper presents an alternative approach to identify and classify the group of small flying objects especially drones from others, notably birds and kites (inclusive of kiteflying), in near field, by examining the pattern of their flight paths and trajectories. The trajectories of the drones and other flying objects were extracted from multiple clips of videos including various natural and synthetic database. Four trajectories characteristics are observed and extracted from the object's flight paths, i.e., heading or turning angle, curvature, pace velocity, and pace acceleration. Subsequently, principal component analyses were applied to reduce the number of these trajectory features from 4 to 2 parameters. Multi-class classification by support vector machine (SVM) with non-linear transformation kernel was used. Multiple classification models were developed by several algorithms with various transformation kernels. The hyperparameters were optimized using Bayesian optimization. The performances of the different models are compared through the prediction accuracy of the test data.

Keywords: drone/birds/kites and others classification, trajectory characteristics, multi-class classification, Bayesian optimization, support vector machine (SVM)

1. Introduction

Small flying objects are those non-aeroplane, non-helicopters and other human-carrying flying machines. They are natural flyers, such as birds, as well as man-made items such as drones, kites and others, which are generally for hobbies, leisure and also professional uses. Operationally, these small flying objects are comparatively tiny in size, and that they are difficult to be detected by conventional means, such as radio-frequency, radar, acoustics, etc. [1, 2]. The most effective way is still largely visual-based [2, 3]. Moreover, even if they are detected, they are difficult to be correctly determined or classified [2].

In this type of small flying object, UAVs referred collectively as drones stand out and gained popularity and a lot of attractions from both amateurs and professionals in recent years. Such popularity has manifested itself as a lot of drones trespassed into prohibited areas. Drones that fly into protected areas such as airports or other key installations can result in disastrous consequences. Therefore, there is dire need for early detection and identification of such small flying objects, before any other subsequent actions can be performed.

Currently, there are a few studies focusing on birds vs drone classifications. There were even dedicated drone-vs-bird detection challenges in 2017 and 2019 [4]. Most of the work presented in that challenges are mostly based on appearance-based neural network and computer vision e.g., [5–11].

However, in reality, there are several other kind of small flying objects of similar size to drones beyond birds, such as kites, balloons, floating lanterns, etc. Of particular interests are kites, inclusive of kiteflying and parasails, which are quite popular in many parts of the world. As the kites are usually less regulated, kites are more common and are sighted more in the open areas and, in certain cases, they could be in the vicinity of the airport. Besides, from a distance, these kites appeared almost the same as shown in **Fig. 1**. Although, kites and birds may not be a threat, they can cause confusion to any visual-based drone detection, creating false alarm and misinterpretation of the drone, thereby reducing the efficacy of any drone detection. Hence, this leads to the current dedicated focus by Civil Aviation Authority of Singapore (CAAS) [a] and is the main objective of this work.

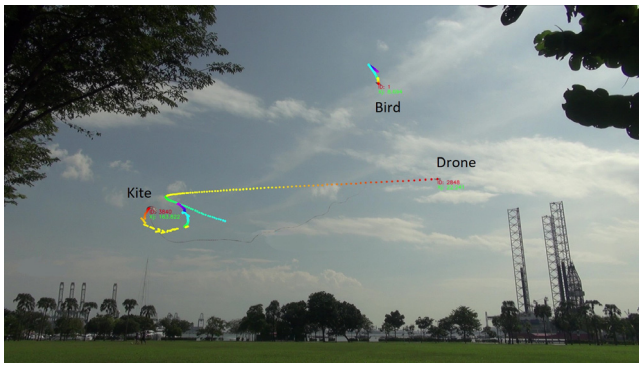

Fig. 1. Drone, bird and kite in flights. Their trajectories are shown with rainbow color (see Section 3).

Despite this fact, there are no dedicated studies on classification of drones vs. kites to date as compared to drones vs. birds, to the authors' knowledge. Hence, this work aims to fill in such gap by identifying drones from both birds and kites collectively. These will further benefit the airport community so as to be able to provide more accurate identification and prevent intrusion with fewer errors.

In this paper, we present a unified method of classifying small flying objects to be drones, birds, kites, and others. As these objects are very small in size, we propose to do so by focusing on their trajectories (flight paths) instead of their appearances. This trajectory-based classification method to identify drones from birds was initially proposed in our preliminary work in [12]. That previous work was based on a binary support vector machine classifier. Here, we extend further to include multi-class classification and the usage of several classifiers for drones, birds, and kites classification.

Therefore, the main contribution and novelty of the paper are the classification of small flying objects which are drones, birds, and other flying objects (e.g., kites), by using our proposed flight kinematic feature and support vector machine. Notwithstanding that, to the authors' knowledge, this has not been done before. Also, for the tiny flying objects, the appearance-based technique will not be practical as the images would be too small and lead to false detection.

2. Trajectory Characteristics

The trajectory-based classification is based on the physio-biological behavior of the flying objects. One can use the unique features of these flying objects as characteristics (features). This trajectory-based technique could be an effective alternative method from the typical appearance-based, and is suitable for video surveillance, as one can simply extract the path with time history, from either radars, cameras, or other visual tools. The technique is not limited to the camera nor lens capabilities. A prior attempt was done by Thai et al. [13] on trajectory detection on drone vs. airplane.

Here, we propose to examine the following trajectory features, i.e., 1) turning (heading) angle, 2) curvature, 3) object pace velocity, and 4) object pace acceleration. **Fig. 2** shows the schematic diagram of an arbitrary trajectory and the definitions of these trajectory characteristics.

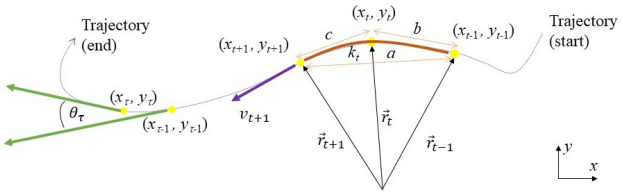

Fig. 2. Schematic diagram of an arbitrary trajectory showing definitions of trajectory characteristics.

2.1. Turning (Heading) Angle, θ_t

The heading turning angle θ_t infers how the flying object changes its direction during its course of flight. For typical small drones, its flight should be straighter and more steady. The small drone can have either a small sharp turning angle during its course or large turning angle during an occasional turn, whereas for other flying objects, their turning angles can be moderately large.

The flight path trajectory of the flying object can be created by connecting the tracked positions of such flying object at each frame, as shown in diagram in **Fig. 2**. The turning angle θ_t can also be calculated from two positions from two consecutive time step as shown in Eqs. (1) and (2). The turning direction in which the object flew is trivial, i.e., objects that fly from left to right are treated the same as an object flying from right to left. Therefore, the absolute value of θ_t is used.

$$\theta_t = \tan^{-1} \frac{y_t - y_{t-1}}{x_t - x_{t-1}}, \quad \ldots\ldots\ldots\ldots (1)$$

$$\Delta\theta_t = \theta_t - \theta_{t-1}, \quad \ldots\ldots\ldots\ldots (2)$$

where (x_t, y_t) is an object position at time frame t.

Throughout the flights, the flying objects might do various turns along their courses, therefore, the average value of θ_t, defined below is used.

$$\theta_{avg} = \frac{1}{T} \sum_{t=1}^{T} \theta_t. \quad \ldots\ldots\ldots\ldots (3)$$

2.2. Curvature, κ_t

The curvature κ measures the amount by which a flight path deviates from being a straight line. The curvature of a straight line is zero. It is used in conjunction to the turning angle feature. For drones, as the flight contains more straight portion, the average curvature should be close to zero, whereas for birds and kites, their flight paths are more curvy or periodic, and the average curvature is of certain positive value. The curvature is simply the angle between the two lines connecting three consecutive points. Curvature is calculated by using three consecutive

frames.

$$\kappa_t = \cos^{-1}\frac{a^2-b^2-c^2}{2bc}, \quad \ldots\ldots\ldots\ldots (4)$$

where a, b, c are Euclidean distances from (x_{t+1}, y_{t+1}) to (x_{t-1}, y_{t-1}), from (x_t, y_t) to (x_{t-1}, y_{t-1}) and from (x_{t+1}, y_{t+1}) to (x_t, y_t). Similar to the turning angle θ_t, this feature is invariant with turning direction, and the average value of κ_t is used.

2.3. Object Pace, v_t

The pace of the flying object here refers to the object's velocity and acceleration. Considering the trajectory of each of the flying object, the spacing or the segment length between two positions represents the distance travelled by the same flying object between the two time, i.e.,

$$\overrightarrow{\Delta r} = \overrightarrow{r}_{t+1} - \overrightarrow{r}_t. \quad \ldots\ldots\ldots\ldots (5)$$

As almost all the cameras have fixed shuttle speed or frame rate, the time between two positions Δt are constant. Hence, we can estimate the speed of the flying object, from the segment lengths, i.e.,

$$v_t = \frac{\mathrm{d}r}{\mathrm{d}t} \sim \left|\frac{\overrightarrow{\Delta r}}{\Delta t}\right| \sim \frac{r_t - r_{t-1}}{\Delta t}. \quad \ldots\ldots\ldots (6)$$

2.4. Accelerations of the Flying Object, a_t

Similarly, the accelerations of the flying object can be estimated from the trajectory. If the flying object accelerates, the two consecutive segment lengths will increase. The acceleration can be estimated from:

$$a_t = \frac{\mathrm{d}^2 r}{\mathrm{d}t^2} \sim \frac{r_{t+1} - 2r_t + r_{t-1}}{\Delta t^2}. \quad \ldots\ldots\ldots (7)$$

The acceleration can be positive and negative, corresponding to speed-up and slow-down motions. Here the magnitudes (absolute values) of v_t and a_t are used.

These velocity and acceleration parameters, v_t and a_t can be used as features to classify trajectories of the drones from the other flying objects. For drones' flights, as the drones are practically able to accelerate and decelerate more easily and rapidly, their flight paths could have variable paces, manifested as variable segment lengths. On the other hand, the birds and kites fly at relatively high but mostly constant speeds [14] most of the time. Moreover, both birds and kites' accelerations are comparatively low, their flight paths could have more constant paces, manifested as regular segment lengths.

Like θ_t and κ_t, the average values of v_t and a_t are used.

3. Methodology

In this section, we revisit the principles of the three main tools that we used: 1) binary classification model selection using Bayesian optimization, 2) principal component analysis (PCA), and 3) multi-class classifications.

3.1. Binary Classification Model Selection Using Bayesian Optimization

We started the work by designing the machine learning models to do simple threshold-based binary classification of drones vs. others (combining birds, kites and other small flying objects). There are several algorithms to do such binary classifications. Here, we select the established and popular models, i.e., support vector machines (SVMs), decision tree, ensemble of decision trees, and naive Bayes model [b].

Assuming linearly separable data, the SVM minimizes the objective function:

$$\min_{\beta,b}\left(\frac{1}{2}\|\beta\| - \sum_j \alpha_j\left(y_j\left(x'_j\beta + b\right) - 1\right)\right), \quad . \quad (8)$$

where x_j is the j-th data point, and y_j is the label $\{+1, -1\}$ of the x_j corresponding to drones and birds trajectories respectively, β is the normal vector to the separating hyperplane, b is the bias, and α_j is a non-negative Lagrange multiplier enforcing the classification constraint.

The margin γ, defined by $2/\|\beta\|$ defines the maximal distance normal to the hyperplane with no interior data points. A larger margin is indicative of better class separability.

3.2. Principal Component Analysis (PCA)

Principal component analysis (PCA) is introduced to extract representative features in the dataset. The concept is excerpted here. PCA assumes the cross-correlation in all these trajectory features and exploits it to extract unique features, known as principal components which maximize the variances in the new feature space [15].

These inherent correlations are exploited to find principal components which are linear combinations of the original input data. The k-th principal component (PC) z_k is given by

$$z_k = \sum \alpha_k \hat{I} = \alpha_{k1}\hat{I}(\theta) + \alpha_{k2}\hat{I}(\kappa) + \alpha_{k3}\hat{I}(v) + \alpha_{k4}\hat{I}(a), \quad \ldots\ldots\ldots\ldots (9)$$

where $\hat{I}(\theta)$, $\hat{I}(\kappa)$, $\hat{I}(v)$, $\hat{I}(a)$ are the normalized turning angle, curvature, pace velocity, and pace acceleration measured, and α_k is the feature vector of the k-th PC, which has unit length (i.e., $\|\alpha_k\| = 1$).

The k-th PC is derived from the singular-value decomposition or the eigenvectors of the covariance matrix $\mathbb{C}$ where

$$\mathbb{C} = \frac{\hat{I}\hat{I}^T}{N}. \quad \ldots\ldots\ldots\ldots (10)$$

The k-th column of $P = [\alpha_1, \alpha_2, \alpha_3, \alpha_4]$, α_k contains the coefficients of the k-th PC and corresponding eigenvalue, indicates the relative order of the PCs. N is the sample size. Significantly, the eigenvector with the highest associated eigenvalue is the 1st PC. The variance of the k-th

PC is defined as

$$\sigma_{zk} = \frac{1}{N-1}\sum_{i=1}^{N}\left|z_{k,1} - \bar{z}_k\right|^2, \quad \ldots\ldots\ldots (11)$$

where N is the sample size, and $\bar{z}_k$ is the sample mean. The variances of the original θ, κ, v, t components prior to the PCA transform are denoted as σ_θ, σ_κ, σ_v, and σ_t respectively [16].

3.3. Multi-Class Classification Model Selection Based on Support Vector Machines

In this work, we aim to classify the flying objects either as drones, birds and other (mainly kites). This is multi-class classification problem. The expanded support vector machine (SVM) can be applied. A multi-class SVM constructs a hyper-plane or set of hyper-planes in a high or infinite dimensional space, which can be used for classification, regression or other tasks [17]. A good separation is achieved by the hyper-plane that has the largest distance to the nearest training data points of any class (functional margin), since in general the larger the margin the lower the generalization error of the classifier. Four sub-types of SVM models are used [18]: 1) support vector classification (SVC) with linear kernel, 2) linear SVC, 3) SVC with radial-basis function (RBF) kernel, and 4) SVC with polynomial kernel. Here are the brief summary of these models [19].

3.3.1. Support Vector Classifications (SVC) with Linear Kernel

Given training vectors $x_i \in \mathbb{R}^p$, $i = 1,\ldots,n$ in two classes, and a vector $y \in \{1,-1\}^n$, the goal is to find $w \in \mathbb{R}^p$ and $b \in \mathbb{R}$ such that the prediction given by $\text{sign}\{w^T\phi(x)+b\}$ is correct for most samples. SVC solves the following primal problem:

$$\min_{w,b,\xi} \frac{1}{2}w^T w + C\sum_{i=1}^{n}\xi_i, \quad \ldots\ldots\ldots (12)$$

subject to $y_i\{w^T\phi(x_i)+b\} \geq 1-\xi_i$ and $\xi_i \geq 0$, $i = 1,\ldots,n$.

In principle, one can maximize the margin (by minimizing $||w||^2 = w^T w$), while incurring a penalty when a sample is misclassified or within the margin boundary. Ideally, the value $y_i\{w^T\phi(x_i)+b\} \geq 1$ for all samples indicates a perfect prediction. But problems are usually not always perfectly separable with a hyperplane, so we allow some samples to be at a distance ξ_i from their correct margin boundary. The penalty term C controls the strength of this penalty, and as a result, acts as an inverse regularization parameter. The dual problem to the primal is

$$\min_{\alpha} \frac{1}{2}\alpha^T Q\alpha - e^T\alpha, \quad \ldots\ldots\ldots (13)$$

subject to $y^T\alpha = 0$ and $0 \leq \alpha_i \leq C$, $i = 1,\ldots,n$, where e is the vector of all ones, and Q is an $n \times n$ positive semidefinite matrix, $Q_{i,j} \equiv y_i y_j K(x_i,x_j)$, where $K(x_i,x_j) = \phi(x_i)^T\phi(x_j)$ is the kernel. The terms α_i are the dual coefficients, and they are upper-bounded by C. This dual representation highlights the fact that training vectors are implicitly mapped into a higher (maybe infinite) dimensional space by the function ϕ. Once the optimization problem is solved, the output of decision function for a given sample x becomes:

$$\sum_i y_i\alpha_i K(x_i,x) + b, \quad \ldots\ldots\ldots (14)$$

and the predicted class corresponds to its sign. We only need to sum over the support vectors (i.e., the samples that lie within the margin) because the dual coefficients α_i are zero for the other samples.

3.3.2. Linear SVC

The primal problem can be equivalently formulated as

$$\min_{w,b} \frac{1}{2}w^T w + C\sum_{i=1}^{n}\max\left(0,(1-y_i\{w^T * x + b\})\right), \quad (15)$$

where the hinge loss is used. This is the form that is directly optimized, but unlike the dual form, this one does not involve inner products between samples, so the kernel trick cannot be applied, and only the linear kernel is supported.

3.3.3. SVC with Radial-Basis Function (RBF) Kernel

The RBF kernel is a stationary kernel. It is also known as the "squared exponential" kernel. It is parameterized by a length scale parameter $\sigma > 0$, which can either be a scalar (isotropic variant of the kernel) or a vector with the same number of dimensions as the inputs x (anisotropic variant of the kernel). The kernel is given by:

$$K(x_i,x_j) = \exp\left(-\frac{(x_i-x_j)^2}{2\sigma^2}\right), \quad \ldots\ldots\ldots (16)$$

where σ is the length scale of the kernel and $(x_i-x_j)^2$ is the Euclidean distance.

3.3.4. SVC with Polynomial Kernel

For degree-d polynomials, the polynomial kernel is defined as

$$K(x_i,x_j) = (x_i^T x_j + c)^d, \quad \ldots\ldots\ldots (17)$$

where $c \geq 0$ is a free parameter trading off the influence of higher-order versus lower-order terms in the polynomial. When $c = 0$, the kernel is called homogeneous.

4. Experiment and Results

4.1. Flight Trajectory Dataset and Image Acquisition

In this work, the training data set consists of 52 videos of drones and swarm of birds in flight. The 52 clips can be further broken down into 24 clips of only birds, 18 clips of only drones, and 10 clips of only kites. There are 2 video

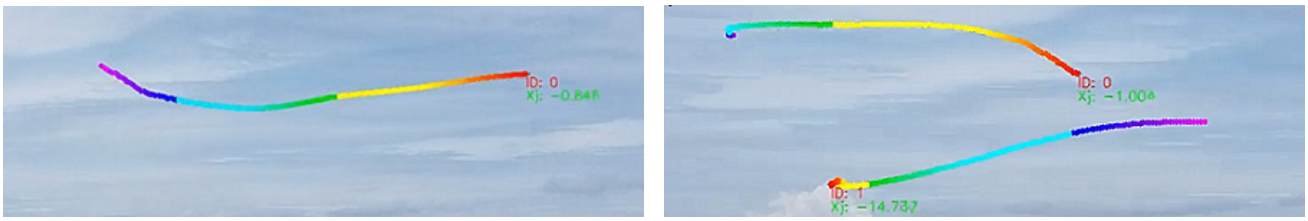

(a) (b)

Fig. 3. Sample snapshot from the video clip of two tracked drones with their trajectories.

(a) (b)

Fig. 4. Snapshot from the video clip of the two tracked drones flying above one tracked bird below with their trajectories.

(a) (b)

Fig. 5. Snapshot from the video clip of the tracked kite with its trajectory.

clips with a mixture of drones, birds and kites for testing. All the video clips were captured from a static camera with a fixed angle of view to minimize the ambiguity from the camera's own motions. The flight test data were from 1) our own flights of small drones, and 2) publicly available moving clips of flocks of flying birds. The drone's flights and mixtures of drones, birds and kites were from our own open field tests, whereas the birds and kites in flights were from open source data sources and from the observations of the public kite flyers [c–f].

These video clips ranged from 211 frames to 6000 frames, where the flying objects were tracked for a minimum of 211 frames to a maximum of 5709 frames with the average being 1500 frames in their respective videos. In each frame, there are multiple tracks of birds and drones but only tracks that are at least 10 frame old are considered.

Figures 3(a) and **(b)** show the snapshots from the video clip of the two tracked drone with its trajectory. Likewise, **Figs. 4(a)** and **(b)** show the snapshots from the video clips of the two tracked drones flying above one tracked bird with their trajectories. **Figs. 5(a)** and **(b)** show the snapshot from the video clip of one tracked kite with its trajectory. In these three figures, the different shades of these trajectories indicate the age, of which the lighter shade means the newest and the darker shade means the oldest. **Figs. 6** and **7** show the snapshot from the video clip of the swarm of birds with their trajectories. In total, there were 41337 frames which contained 1302 tracks (388 for drones, 804 for birds, and 110 for kites).

Table 1 shows the average trajectories characteristics data from observed 1302 tracks for drones, birds and kites. The drone tracks show distinctively high turning (bending angles), high curvatures, high pace velocities and accelerations. This is expected due to their agility and high maneuverability.

The bird tracks show smaller average turning angle and curvatures compared to drones by more than half. This shows the bird flights are relatively more smooth trajectories than those of the drones. The kite tracks are somewhat between the birds and the drones in heading angles and curvatures, but with significantly lower pace velocities as they are mostly tethered and stay relatively in one fixed positions.

Fig. 6. Snapshot from the video clip of the swarm of birds (left) and with detection (right).

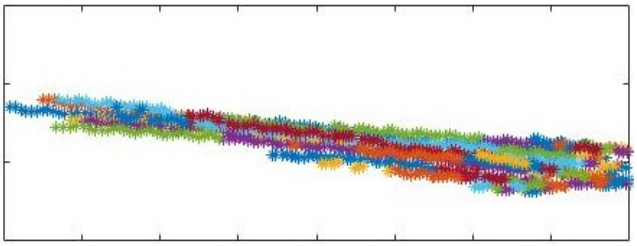

Fig. 7. Trajectories of the swarm of birds trajectory, as in **Fig. 6**.

Table 1. Trajectories characteristics: observed average data.

Flight	Number of tracks observed	Angle θ_t [deg]	Curve κ_t [deg]	Vel. v_t [pixel]	Acc. a_t [pixel]
Drone	388	18.41	28.37	10.46	0.08
Bird	804	9.29	12.53	3.94	0.01
Kite	110	14.83	16.10	0.64	0.01

We can use the results from **Table 1** as a basis for classification of whether the detected and tracked flying objects are the drones or others. The next section will discuss the scheme for general binary classifications, i.e., drone vs. others (birds and kites combined). The subsequent section will discuss more specific scheme for multi-class classifications, i.e., drone, birds and kites.

4.2. Binary Classification Results

We built multiple classification models for the training data set as shown in **Table 1**, optimizing the hyperparameters using Bayesian optimization and selecting the model that performs the best on the test data set. As Bayesian optimization finds an optimal set of hyperparameters for a given model by minimizing the objective function of the model, the algorithms are optimized and we get the optimal set of hyperparameters.

In this work, we use MATLAB Statistics and Machine Learning Toolbox [b]. We customize the hyperparameter optimization options, run Bayesian optimization in parallel, fit the training data set and tune the parameters. We extracted the Bayesian optimization results from each model and plot the minimum observed value of the objective function for each model over every iteration of the hyperparameter optimization. The objective function value corresponds to the misclassification rate measured by five-fold cross-validation using the training data set. The result is shown in **Fig. 8(a)**. The corresponding confusion matrix on the test set is shown in **Fig. 9**.

Based on the confusion matrix, the ensemble of decision trees and SVM models achieve correct prediction, therefore we continue running Bayesian optimization on these 3 models. The plot of total minimum observed values of the objective function for each iteration of Bayesian optimization of SVMs and decision trees models are shown in **Fig. 8(b)**.

4.3. Principal Component Analysis (PCA) Results

The 3 features derived from trajectories of the flying objects with 4 parameters allow the differentiation between the drones and birds' flight. Principal component analyses (PCA) was applied to reduce the parameters down to 2 new features for subsequent classification. With feature extraction and dimension reduction, the new features are separated each other for further classification by support vector machine (SVM).

A MATLAB function *pca* from Dimensionality Reduction and Feature Extraction Toolbox are used in this work [g]. Here, PCA is applied to the dataset as presented in Section 3. The PCA result is shown in **Fig. 10**. The corresponding coefficients P and the eigenvalues of the k-th PC are shown in **Tables 2** and **3** respectively.

4.4. SVM Results

From the previous binary classification section, SVM models provided better prediction for binary classification (drone and others). In this section, we expand SVM models with various kernels to do multi-class classification, i.e., drones, birds and kites using python with SciKit-Learn library [h]. **Figs. 11(a)–(d)** show the results from SVMs with different kernels as presented, i.e., SVC with linear kernel, linear SVC, SVC with RBF kernel, and SVC with polynomial (degree 3).

Regarding the multi-class classification using SVM, we use the default values for the parameters provided by the SciKit-Learn library as shown in the **Table 4**.

The regularization parameter is kept constant for the different kernels. Only the RBF kernel and the polynomial kernel require the kernel coefficient. It is set to 'scale,' which is set based on the training data provided. As we are training both models using the same data, the kernel coefficient will be set to the same value. For the polynomial kernel, the polynomial degree is set to 3 which provides a balance between complexity and computational time.

As the distance is measured in pixels, objects that are further away will appear to have smaller velocity and acceleration. However, this work focuses on finding key features in 2D images which appeared in the observed camera (2D) that are significant in trajectory classification. With our proposed feature and classification, we are able to classify trajectory of bird, drone and kite at up to 200 m without distance information. To confirm this, we

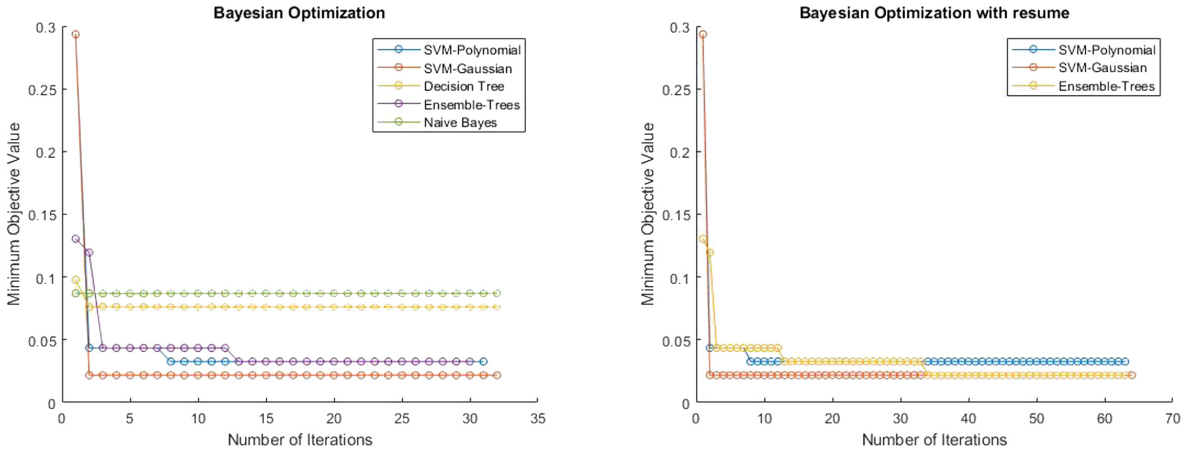

(a) (b)

Fig. 8. (a) Bayesian optimization of classification models, (b) total Bayesian optimization of chosen classification models.

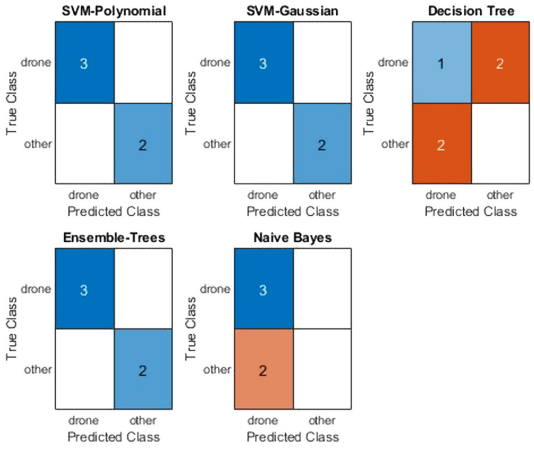

Fig. 9. Confusion matrix of classification models.

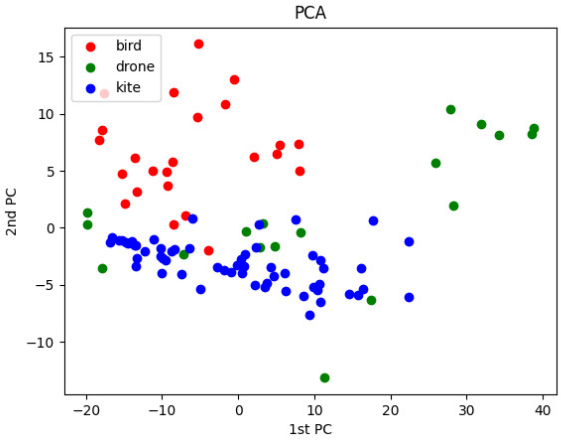

Fig. 10. Scattered plot of drone, bird and kites trajectories on principal components.

Table 2. Coefficients P of the k-th principle component (PC).

θ	κ	v	a
54.13677357	71.98197064	−10.65006283	0.80276533
71.98197064	150.1320662	2.41055688	0.37915395
−10.65006283	2.41055688	20.19399796	−0.66619646
0.80276533	0.37915395	−0.66619646	7.14990225

Table 3. Eigenvalues of the k-th principle component (PC).

1st	2nd	3rd	4th
188.7043	28.68	7.1142	0.0100

conducted tests to check the accuracy in our database at different distance as shown in **Table 5**.

Moreover, even though the velocity and acceleration of an object are described in the unit of pixels, the SVM model will determine the relationship between the different features and assign weights to the features that maximize the separation of the different classes.

The SVM with linear kernel appears to be the best fit with the current data set. The other kernels seem to overfit the data, which may be due to the small training data set. In all these models, the drones are clearly segregated as shown in upper right quadrants. The models could also classify the birds and kites, yet there are overlapped areas. Nevertheless, with the current model, we achieve the objective of identifying and classifying drones, birds and kites. The visual example of the correct classification by SVM with this linear kernel is shown in **Fig. 12(a)**, which is the same as **Fig. 1**. Likewise, for comparison, the visual example of the wrong classification by decision tree (from binary classification in Section 4.2) is shown in **Fig. 12(b)**.

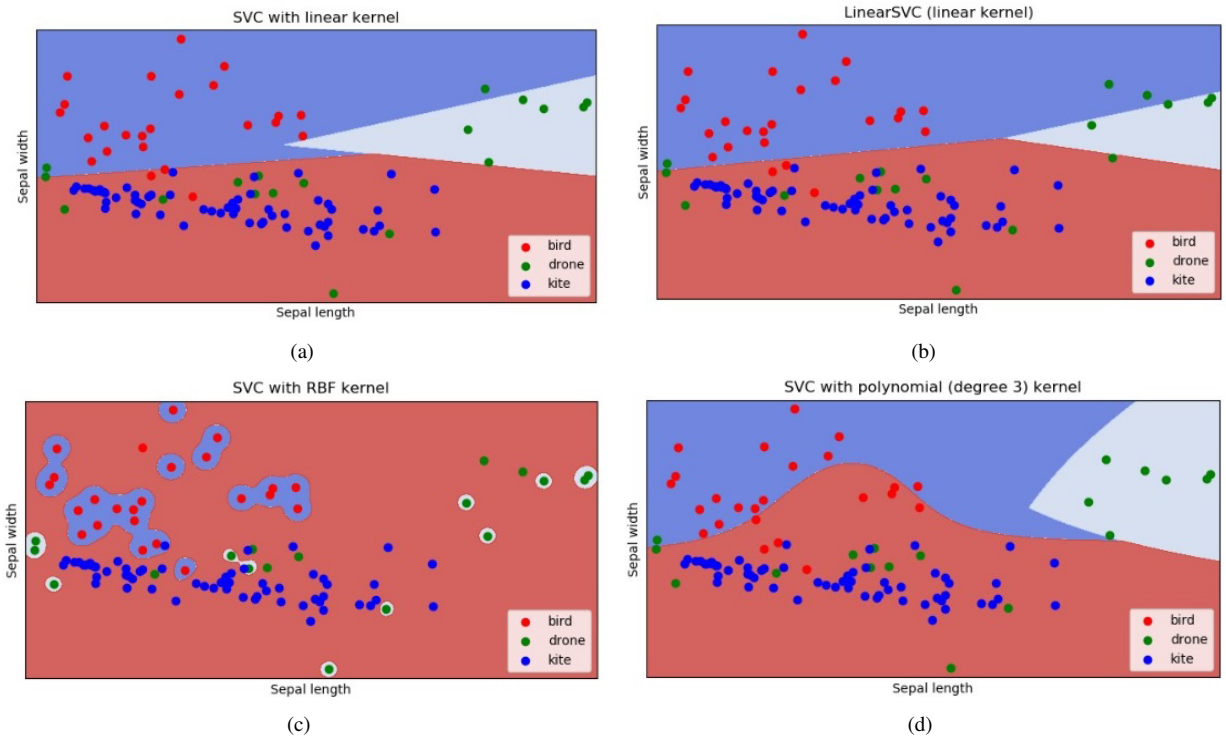

Fig. 11. Results from multi-class linear support vector classification with different kernels.

Table 4. Selection of parameters for support vector machines models.

	Regularization parameter, C	Kernel coefficient, γ	Polynomial degree
SVC with linear kernel	1	–	–
Linear SVC	1	–	–
SVC with RBF kernel	1	scale	–
SVC with Polynomial	1	scale	3

Table 5. SVM prediction accuracy at various distance.

Distance	Accuracy (TP+TN)/(TP+TN+FP+FN)
Up to 20 m	100%
20–100 m	90%
100–200 m (visual detection limit)	80%
Overall	85% (average)

TP: True Positive, TN: True Negative, FP: False Positive, FN: False Negative

5. Conclusion and Future Works

This paper presents an alternative way to identify the small flying object whether it is a drone, a bird or a kite by examining its flight path. The characteristics based on the trajectory are: turning angle (heading), curvature, and pace. These parameters are further reduced by means of PCA to 2 principal features. Subsequently, SVM classification with different kernels were performed and tested. The hyperparameters were optimize a using Bayesian optimization. The performance are compared by prediction accuracy of the test data. The multi-class classification SVM with linear kernel appears to be the best fit with the current data set. The next steps of this work are to collect more datasets either from pre-recorded movie clips or from actual field recordings, and to expand to cover other type of small flying object, e.g., balloon, as well as to include the large flying objects, i.e., airplane and helicopters.

(a) (b)

Fig. 12. Visual example of (a) correct classification for kite, bird and drone by SVM with linear kernel method and (b) wrong classification by decision tree method (kite classified as 'drone').

Acknowledgements

This research was supported in part by Civil Aviation Authority of Singapore (CAAS) and Defense Science and Technology Agency (DSTA), as well as Mohamed Bin Zayed International Robotics Challenge (MBZIRC) Grant. This research is also supported in-part by the Fund for the Promotion of Joint International Research (Fostering Joint International Research (B)) No. 20KK0086.

References:

[1] X. Shi, C. Yang, W. Xie, C. Liang, Z. Shi, and J. Chen, "Anti-drone system with multiple surveillance technologies: Architecture, implementation, and challenges," IEEE Communications Magazine, Vol.56, No.4, pp. 68-74, 2018.

[2] I. Guvenc, F. Koohifar, S. Singh, M. L. Sichitiu, and D. Matolak, "Detection, tracking, and interdiction for amateur drones" IEEE Communications Magazine, Vol.56, No.4, pp. 75-81, 2018.

[3] M. M. Azari, H. Sallouha, A. Chiumento, S. Rajendran, E. Vinogradov, and S. Pollin, "Key technologies and system trade-offs for detection and localization of amateur drones," IEEE Communications Magazine, Vol.56, No.1, pp. 51-57, 2018.

[4] A. Coluccia, A. Fascista, A. Schumann, L. Sommer, M. Ghenescu, T. Piatrik, G. De Cubber, M. Nalamati, A. Kapoor, M. Saqib, N. Sharma, M. Blumenstein, V. Magoulianitis, D. Ataloglou, A. Dimou, D. Zarpalas, P. Daras, C. Craye, S. Ardjoune, D. De la Iglesia, M. Mández, R. Dosil, and I. González, "Drone-vs-bird detection challenge at IEEE AVSS2019," 2019 16th IEEE Int. Conf. on Advanced Video and Signal Based Surveillance (AVSS), pp. 1-7, 2019.

[5] A. Rozantsev, V. Lepetit, and P. Fua, "Flying objects detection from a single moving camera," Proc. of the IEEE Conf. on Computer Vision and Pattern Recognition, pp. 4128-4136, 2015.

[6] F. Gökçe, G. Üçoluk, E. Şahin, and S. Kalkan, "Vision-based detection and distance estimation of micro unmanned aerial vehicles," Sensors, Vol.15, No.9, pp. 23805-23846, 2015.

[7] R. Yoshihashi, T. T. Trinh, R. Kawakami, S. You, M. Iida, and T. Naemura, "Differentiating objects by motion: joint detection and tracking of small flying objects," arXiv preprint, arXiv:1709.04666, 2017.

[8] C. Aker and S. Kalkan, "Using deep networks for drone detection," 2017 14th IEEE Int. Conf. on Advanced Video and Signal Based Surveillance (AVSS), pp. 1-6, 2017.

[9] M. Saqib, S. D. Khan, N. Sharma, and M. Blumenstein, "A study on detecting drones using deep convolutional neural networks," 2017 14th IEEE Int. Conf. on Advanced Video and Signal Based Surveillance (AVSS), pp. 1-5, 2017.

[10] D. H. Ye, J. Li, Q. Chen, J. Wachs, and C. Bouman, "Deep learning for moving object detection and tracking from a single camera in unmanned aerial vehicles (UAVs)," Electronic Imaging, Vol.2018, No.10, pp. 466-1-466-6, 2018.

[11] A. Schumann, L. Sommer, J. Klatte, T. Schuchert, and J. Beyerer, "Deep cross-domain flying object classification for robust UAV detection," 2017 14th IEEE Int. Conf. on Advanced Video and Signal Based Surveillance (AVSS), pp. 1-6, 2017.

[12] S. Srigrarom, K. H. Chew, D. M. Da Lee, and P. Ratsamee, "Drone versus bird flights: Classification by trajectories characterization," Proc. of 2020 59th Annual Conf. of the Society of Instrument and Control Engineers of Japan (SICE), 2020.

[13] V.-P. Thai, W. Zhong, T. Pham, S. Alam, and V. Duong, "Detection, tracking and classification of aircraft and drones in digital towers using machine learning on motion patterns," 2019 Integrated Communications, Navigation and Surveillance Conf. (ICNS), pp. 1-8, 2019.

[14] T. Alerstam, M. Rosén, J. Bäckman, P. G. P. Ericson, and O. Hellgren, "Flight speeds among bird species: allometric and phylogenetic effects," PLoS Biol., Vol.5, No.8, e197, 2007.

[15] J. De Leeuw, "Nonlinear principal component analysis and related techniques," UCLA Department of Statistics Papers, 2011.

[16] I. T. Jolliffe, "Principal component analysis," Springer, 2002.

[17] C. M. Bishop, "Pattern recognition and machine learning," Springer, 2006.

[18] K. Crammer and Y. Singer, "On the algorithmic implementation of multiclass kernel-based vector machines," J. of Machine Learning Research, Vol.2, pp. 265-292, 2001.

[19] A. J. Smola and B. Schölkopf, "A tutorial on support vector regression," Statistics and Computing, Vol.14, No.3, pp. 199-222, 2004.

Supporting Online Materials:

[a] Civil Aviation Authority of Singapore (CAAS), "Steering your aerial activities clear of the airport." https://www.caas.gov.sg/public-passengers/aerial-activities [Accessed October 1, 2020]

[b] MathWorks, "Moving towards automating model selection using Bayesian optimization." https://ww2.mathworks.cn/help/stats/towards-automating-model-selection.html [Accessed September 17, 2020]

[c] Shutterstock, "Birds flying royalty-free stock footage." https://www.shutterstock.com/video/search/birds-flying [Accessed May 5, 2020]

[d] IstockGettyImage, "Flock of birds footage." https://www.istockphoto.com/videos/flockbirds?phrase=flock%20birdssort=mostpopular [Accessed May 5, 2020]

[e] Videezy, "Kite Stock Video Footage." https://www.videezy.com/free-video/kite [Accessed September 17, 2020]

[f] Shutterstock, "Birds flying royalty-free stock footage." https://www.shutterstock.com/video/search/kite [Accessed September 17, 2020]

[g] MathWorks, "Principal component analyses." https://www.mathworks.com/help/stats/principal-component-analysis-pca.html [Accessed April 28, 2020]

[h] SciKit-Learn, "Support vector machines." https://scikit-learn.org/stable/modules/svm.html [Accessed September 18, 2020]

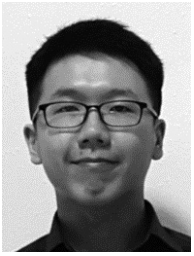

Name:
Jalvin Jia Xiang Chan

Affiliation:
Undergraduate Student, National University of Singapore

Address:
21 Lower Kent Ridge Road, 119077, Singapore

Brief Biographical History:
2017- Department of Mechanical Engineering, National University of Singapore

Name:
Sutthiphong Srigrarom

Affiliation:
Senior Research Scientist, Temasek Laboratories, National University of Singapore

Address:
5A Engineering Drive 1, #09-02 117411, Singapore

Brief Biographical History:
2002- Assistant Professor, Nanyang Technological University
2012- Associate Professor, Singapore Institute of Technology, University of Glasgow
2019- Temasek Laboratories, National University of Singapore

Main Works:
• S. Srigrarom, S. M. Lee, M. Lee, F. Shaohui, and P. Ratsamee, "An integrated vision-based detection-tracking-estimation system for dynamic localization of small aerial vehicles," 2020 5th Int. Conf. on Control and Robotics Engineering (ICCRE), pp. 152-158, 2020.

Membership in Academic Societies:
• The Institute of Electrical and Electronic Engineers (IEEE)
• American Institute of Aeronautics and Astronautics (AIAA)

Name:
Jiawei Cao

Affiliation:
Research Scientist, Temasek Laboratories, National University of Singapore

Address:
5A Engineering Drive 1, #09-02 117411, Singapore

Brief Biographical History:
2014 Received B.Eng. in Mechanical Engineering from Huazhong University of Science and Technology (HUST)
2018 Received Ph.D. in Mechanical Engineering from National University of Singapore (NUS)

Main Works:
• Multi-agent systems, swarm robotics, bio-inspired control and soft robotics

Name:
Pengfei Wang

Affiliation:
Research Scientist, Temasek Laboratories, National University of Singapore

Address:
5A Engineering Drive 1, #09-02 117411, Singapore

Brief Biographical History:
2012 Received Bachelor of Engineering from Huazhong University of Science and Technology
2016 Received Ph.D. from Mechanical Engineering, National University of Singapore

Main Works:
• Sense and avoid of UAVs, deep learning based detection and depth estimation on UAV platform

Name:
Photchara Ratsamee

Affiliation:
Assistant Professor, Cyber-Media Center, Osaka University

Address:
5-1 Mihogaoka, Ibaraki, Osaka 567-0047, Japan

Brief Biographical History:
2012 Received M.E. from Graduate School of Engineering Science, Osaka University
2015 Received Ph.D. from Graduate School of Engineering Science, Osaka University

Main Works:
• Robot vision, human robot interaction, augmented reality, and rescue robot